An optimized cluster density matrix embedding theory

Hao Geng(耿浩) and Quan-lin Jie(揭泉林)

Citation: Chin. Phys. B, 2021, 30 (**9**): 090305. DOI: 10.1088/1674-1056/ac0cdc
Journal homepage: http://cpb.iphy.ac.cn; http://iopscience.iop.org/cpb

What follows is a list of articles you may be interested in

Quantum speed limit for the maximum coherent state under the squeezed environment

Kang-Ying Du(杜康英), Ya-Jie Ma(马雅洁), Shao-Xiong Wu(武少雄), and Chang-Shui Yu(于长水)
Chin. Phys. B, 2021, 30 (**9**): 090308. DOI: 10.1088/1674-1056/ac0daf

Entanglement of two distinguishable atoms in a rectangular waveguide: Linear approximation with single excitation

Jing Li(李静), Lijuan Hu(胡丽娟), Jing Lu(卢竞), and Lan Zhou(周兰)
Chin. Phys. B, 2021, 30 (**9**): 090307. DOI: 10.1088/1674-1056/ac0bb3

Introducing the general condition for an operator in curved space to be unitary

Jafari Matehkolaee Mehdi
Chin. Phys. B, 2021, 30 (**8**): 080301. DOI: 10.1088/1674-1056/abe300

Universal quantum circuit evaluation on encrypted data using probabilistic quantum homomorphic encryption scheme

Jing-Wen Zhang(张静文), Xiu-Bo Chen(陈秀波), Gang Xu(徐刚), and Yi-Xian Yang(杨义先)
Chin. Phys. B, 2021, 30 (**7**): 070309. DOI: 10.1088/1674-1056/ac003b

Wave-particle duality relation with a quantum *N*-path beamsplitter

Dong-Yang Wang(王冬阳), Jun-Jie Wu(吴俊杰), Yi-Zhi Wang(王易之), Yong Liu(刘雍), An-Qi Huang(黄安琪), Chun-Lin Yu(于春霖), and Xue-Jun Yang(杨学军)
Chin. Phys. B, 2021, 30 (**5**): 050302. DOI: 10.1088/1674-1056/abeb0f

---

An optimized cluster density matrix embedding theory

Hao Geng(耿浩) and Quan-lin Jie(揭泉林)†

Department of Physics, Wuhan University, Wuhan 430072, *China*

(Received 19 March 2021; revised manuscript received 9 June 2021; accepted manuscript online 21 June 2021)

We propose an optimized cluster density matrix embedding theory (CDMET). It reduces the computational cost of CDMET with simpler bath states. And the result is as accurate as the original one. As a demonstration, we study the distant correlations of the Heisenberg J_1–J_2 model on the square lattice. We find that the intermediate phase ($0.43 \lesssim J_2 \lesssim 0.62$) is divided into two parts. One part is a near-critical region ($0.43 \lesssim J_2 \lesssim 0.50$). The other part is the plaquette valence bond solid (PVB) state ($0.51 \lesssim J_2 \lesssim 0.62$). The spin correlations decay exponentially as a function of distance in the PVB.

Keywords: cluster density matrix embedding theory, distant correlation, Heisenberg J_1–J_2 model

PACS: 03.65.–w **DOI:** 10.1088/1674-1056/ac0cdc

1. Introduction

Distant correlations capture interesting physical properties (for example, phase transitions[1–9] in exotic phases) of the quantum spin system, which is a typical strongly correlated quantum many body system. But as the dimension of the Hilbert space grows exponentially with the system size, it is difficult to solve a large system exactly. An effective and accurate description of large systems would have significant impact on theoretical predictions. Density matrix embedding theory (DMET)[10–14] is a cheap method to map the system to a quantum impurity plus bath problem. The complexity, of the impurity basis construction in DMET, could amount to a rather small matrix diagonalization. However, the DMET still needs remarkable computational cost to simulate large systems, because it needs different configurations to formulate the system.

In this paper, we optimize the cluster density matrix embedding theory (CDMET).[13] In our optimized CDMET, the configurations, of a great part of the system, are treated as identical. This reduces the computational cost. The accuracy is the same as before. The new CDMET we propose in this paper is effective and computationally accessible. It does not deteriorate with the system size. It can be applied to a broad range of problems. We study the validity of the new CDMET by implementing it on the Heisenberg J_1–J_2 model on the square lattice. The Hamiltonian of this model is

$$H = J_1 \sum_{(i,j)} \boldsymbol{S}_i \cdot \boldsymbol{S}_j + J_2 \sum_{\langle i,j \rangle} \boldsymbol{S}_i \cdot \boldsymbol{S}_j \quad (J_1, J_2 > 0), \tag{1}$$

where (i,j) represents the nearest neighbor (NN) and $\langle i,j \rangle$ represents the next nearest neighbor (NNN). For convenience, we set $J_1 = 1$ as the energy unit throughout the paper. We set the lattice spacing between the nearest neighbor spins as the length unit. We define a cluster as a square of 2×2 spins. This shape of cluster is demonstrated to be suitable for application to a square J_1–J_2 lattice.[13] We consider the system with periodic boundary conditions. This model is simple and useful in Fe-based superconductors and other materials.[15] Different theoretical approaches are used to study this model.[13,14,16–29] A well-established consensus is that the model has Neel magnetic long range order at small J_2 region and stripe magnetic long range order at large J_2 region. The combined effect of frustration and quantum fluctuations destroys antiferromagnetism. It leads to a nonmagnetic quantum paramagnetic (disordered) phase (intermediate phase), within the intermediate parameter region. However, two problems of this model are still under debate: the nature of the disordered intermediate phase, and the phase transition between it and the Neel phase. Because of the sign problem, large scale quantum Monte Carlo simulations cannot be applied to these two problems.[30] We think that our new CDMET is a good alternative option to shed light on these two problems. In Refs. [13,14], the Neel phase (a long range order phase) appears at small J_2 values. At $J_2 \sim 0.42$ the system transfers from the Neel phase into a disordered phase. The system undergoes a transition to the stripe phase (another long range order phase) at $J_2 \sim 0.62$. We repeat their results with CDMET.

In the new CDMET, we use a cheap method to treat the remote part of the bath state. The spin energies obtained by the original and the new CDMET are consistent with each other pretty well. By implementing the new CDMET on the large system, we find that the intermediate phase is divided into two parts. One part is a near-critical region ($0.43 \lesssim J_2 \lesssim 0.50$). The other part is the plaquette valence bond (PVB) phase ($0.51 \lesssim J_2 \lesssim 0.62$). In the PVB phase, the spin correlations decay exponentially. After careful observation of the distant spin correlations, the entanglement entropy (EE), and the spin energy, we conclude that the transition from the Neel phase to the intermediate phase is continuous. The small near-critical region ($0.43 \lesssim J_2 \lesssim 0.50$) may be a mixture of the Neel phase

†Corresponding author. E-mail: qljie@whu.edu.cn

and the valence bond solid (VBS) phase (Neel phase with VBS modulation).

2. Formulation

The wave function of CDMET is[13]

$$|\Psi\rangle = \sum_{i=1}^{n_i} a_i |\alpha_i\rangle |\beta_i\rangle, \tag{2}$$

where $\{|\alpha_i\rangle\}$ denotes the basis set of the impurity (the embedded spins), $\{|\beta_i\rangle\}$ denotes the bath (other spins except the embedded spins) states, a_i denotes the expansion coefficient, and n_i denotes the number of impurity basis. The number of the bath states equals the number of the impurity basis. In the original CDMET,[13] the bath state $|\beta_i\rangle$ is block-product state $|\beta_i\rangle = \prod_c |\beta_i^c\rangle$, where $|\beta_i^c\rangle$ denotes the state of bath cluster c. It goes without saying that, in the original CDMET, for any cluster, the n_i states $|\beta_i^c\rangle$ are treated as different.

In our optimized CDMET, for the distant clusters from the embedded spins, the n_i states $|\beta_i^c\rangle$ of a cluster are treated as identical,

$$|\beta_i^c\rangle = |\beta^c\rangle. \tag{3}$$

In the new CDMET, the neighbor clusters of the embedded spins are treated just like in the original CDMET. The distant clusters from the embedded spins are treated as shown in Eq. (3). This formulation simplifies the bath states. It is based on the consideration that the remote clusters have minor influence on the embedded spins. This treatment reduces the computational cost. It lightens the burden in the calculation of large systems. Fan *et al.*[13] noted that the spin energy of the remote clusters is close to that obtained by the hierarchical mean-field method.

The subsequential question is to decide which clusters should be treated as neighbor clusters in the new CDMET. To answer this question, we try some cases (Figs. 1–3) with the new CDMET. We compare the spin energy of an embedded cluster obtained by the original CDMET with that obtained by the new CDMET. In the first case, the clusters (red solid boxes in Fig. 1), which have both J_1 and J_2 interactions with the embedded spins, are treated as neighbor clusters in the new CDMET. In this case, the spin energy is close to the original result (Fig. 2). The spin energy difference between the original and the new CDMET is not obvious at small J_2 values. But at large J_2 region, the difference becomes obvious. In the second case, the clusters (red dashed boxes in Fig. 1), which have only J_2 interactions with the embedded spins, are treated as neighbor clusters in the new CDMET. In this case, the spin energy difference between the new and the original CDMET is obvious at all J_2 values (Fig. 2).

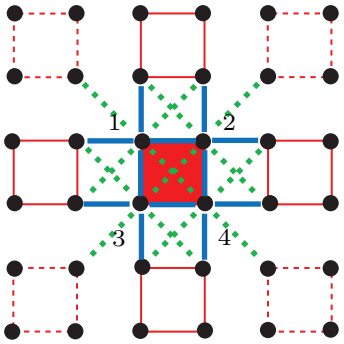

Fig. 1. The black circle dots denote the spins. The blue (green dashed) bonds denote the nearest (next nearest) neighbor interactions. The red shaded box denotes the impurity cluster. The red solid boxes denote the bath clusters which have both J_1 and J_2 interactions with the impurity. The red dashed boxes denote the bath clusters which only have J_2 interactions with the impurity. The embedded spins are numbered from 1 to 4.

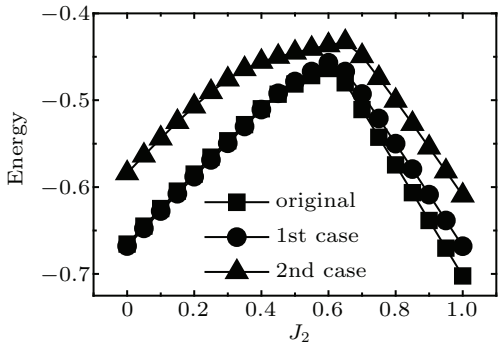

Fig. 2. The spin energy of an embedded cluster, obtained by the original CDMET (squares) and the new CDMET, in a system of 8×8. Two cases in the new CDMET are considered. In the first case (cycles), the clusters, which have both J_1 and J_2 interactions with the embedded spins, are treated as neighbor clusters. In the second case (triangles), the clusters, which have only J_2 interactions with the embedded spins, are treated as neighbor clusters.

In the third case, the clusters (red solid boxes and red dashed boxes in Fig. 1), which have (J_1, J_2) interactions with the emebdded spins, are treated as neighbor clusters in the new CDMET. In this case (Fig. 3), the spin energy obtained by the original CDMET is pretty well consistent with that obtained by the new CDMET. The original CDMET is implemented in the system of 8×8. The new CDMET is implemented in the systems of 8×8, 12×12, 24×24. The largest absolute value of the spin energy differences (Fig. 3(b)) between the new and the original CDMET is about 0.002. The error between different methods seems to be the largest around PVB to stripe phase transition in Fig. 3. As it is a first order phase transition, the wave function has a sudden change. A disturbance may take place around this phase transition. This enlarges the error. Some curves in Fig. 3(a) are shifted. Without shift, the curves in Fig. 3(a) are completely identical. Meanwhile, in the system of 12×12, in the third case, to run a step (calculate all the states and all the clusters once), the new CDMET needs about 1/5–1/4 of the time needed by the original CDMET. Starting from a random initial wave function, we measure the time that the new (original) CDMET needs to get the ground state wave function. At a J_2 value, we try 15 random initial

wave functions, and take the average time T_{new} (T_{original}). The ratio $T_{\text{new}}/T_{\text{original}}$ at $J_2 = 0.2, 0.45, 0.55, 0.80$ are respectively about 0.16, 0.25, 0.22, 0.29. This illustrates the gain in computational efficiency of the new CDMET. The new CDMET reduces the computational cost, and is as accurate as the original CDMET. Furthermore, the spin energies (Fig. 3) obtained by the new CDMET implemented in different system sizes are consistent with each other very well. This indicates that, unlike some other simulation approaches, the new CDMET, as well as the original CDMET,[13] is insensitive to the system size. It can obtain reasonable results in the thermodynamics limit at a finite system size. This allows us to study the system at the thermodynamic limit without further extraneous numerical approximations. However, in the new CDMET, the lack of long-range interactions in the spin lattice model may be a reason for the insensitivity to the system size.

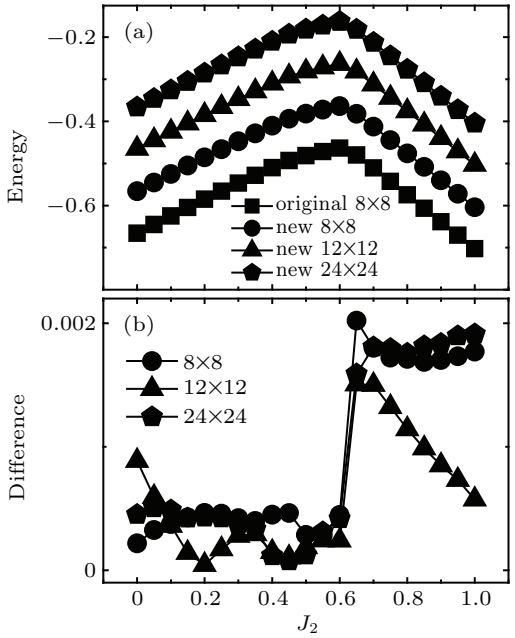

Fig. 3. (a) The spin energy of an embedded cluster, obtained by the original and the new CDMET. The curves of cycles, triangles, pentagons are respectively shifted by 0.1, 0.2, 0.3. Without shift, the four curves are completely identical. (b) The absolute values of the spin energy difference between the original CDMET and the new CDMET. The original CDMET is implemented in the system of 8×8 (squares). The new CDMET is implemented in the systems of 8×8 (cycles), 12×12 (triangles), 24×24 (pentagons).

3. Distant correlation

At first, we briefly introduce the ground state phase diagram (Fig. 4) in this paper. In the small J_2 region ($J_2 \lesssim 0.42$), the ground state has the Neel antiferromagnetic (AF) long range order with a Bragg peak at $q = (\pi, \pi)$ in the spin structure factor. When J_2 is comparable to J_1 ($J_2 \gtrsim 0.63$), the stripe AF long range order, with Bragg peaks at $q = (0, \pi)$ and (π, 0) in the spin structure factor, is stabilized. Between these two long range order phases, there are a near-critical region ($0.43 \lesssim J_2 \lesssim 0.50$) and the PVB ($0.51 \lesssim J_2 \lesssim 0.62$).[16,18,25,29]

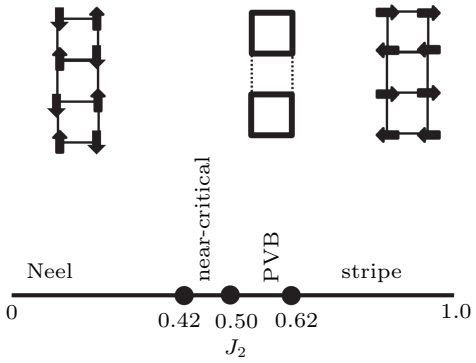

Fig. 4. Ground state phase diagram of Heisenberg J_1–J_2 model on square lattice obtained in the present study.

3.1. The intermediate phase is divided into two parts

The nature of the intermediate phase is still in debate. Many interpretations are proposed, such as spin liquids (SL), valence bond states like the columnar and staggered dimer VBS, the PVB and the plaquette resonating valence bond (PRVB) state.[16,17,19–29] To go deep into this exotic and mysterious phase, we use the new CDMET to embed 6 spins at the top left corner of 6 horizontally consecutive clusters, on a large system (24×24). We calculate spin correlation $C(i, j) = \langle \boldsymbol{S}_i \cdot \boldsymbol{S}_j \rangle$, where $\boldsymbol{S}_i$ and $\boldsymbol{S}_j$ are respectively spin operators of spin i and spin j. In the Neel phase, the spin correlations change with distance in a way far from exponential decaying (Fig. 5(a)). However, when the system comes into the intermediate phase from the Neel phase, the spin correlations gradually tend to decay exponentially. In $0.43 \lesssim J_2 \lesssim 0.50$, the spin correlations decay slower than an exponential one. But, when $J_2 \gtrsim 0.51$ the decaying is exponential. Consistently, Wang *et al.*[31] also found that, in the region $0.572 < J_2 \leq 0.6$, the spin correlations decay exponentially. This subtle change at $J_2 \simeq 0.50$ may indicate a phase transition, which was also noted by Gong *et al.*[16] at $J_2 = 0.5$. We conjecture that the small region $0.43 \lesssim J_2 \lesssim 0.50$ is a near-critical region. It connects the slow decaying region (the Neel phase) with the exponential decaying region ($0.51 \lesssim J_2 \lesssim 0.62$). According to the work of Gong *et al.*,[16] the system is in the PVB phase at $0.5 < J_2 < 0.61$. Consistently, Doretto[29] also agreed that the PVB phase takes place in this region. Subsequent results (Fig. 7) in this paper also indicate that the system is in the PVB phase at $0.51 \lesssim J_2 \lesssim 0.62$.

The small near-critical region ($0.43 \lesssim J_2 \lesssim 0.50$) might be a mixed phase (Neel phase with VBS modulation).[33,34] As we can see that (Fig. 5(a)), in this near-critical region, the spin correlations decay faster than those in the Neel phase, but slower than those in the PVB phase. This region looks like a mixture of the Neel phase and the VBS phase. The change, of the spin correlations (Fig. 5(a)) from $J_2 = 0.4$ to $J_2 = 0.55$ is gradual. This indicates that the controversial phase transition[20,32] from the Neel phase to the intermediate phase is continuous.

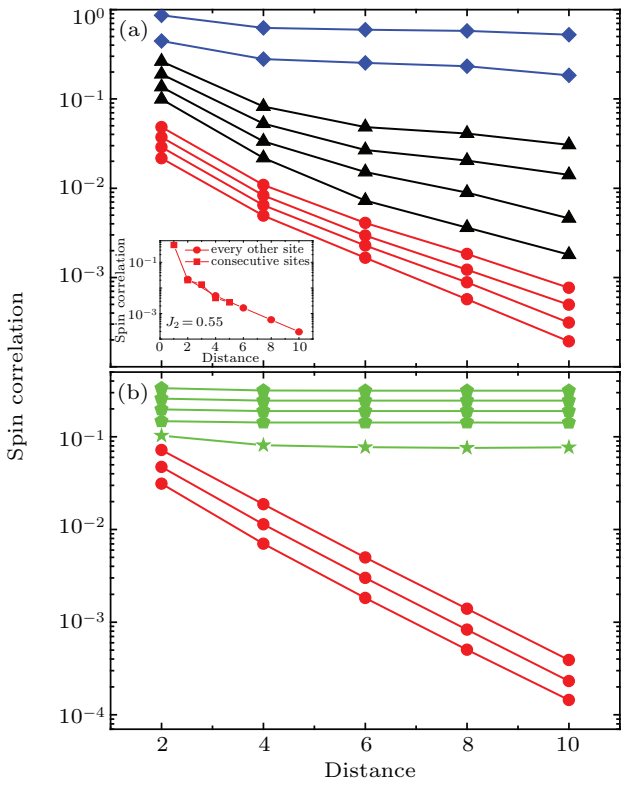

Fig. 5. Absolute values of spin correlations obtained from the new CDMET in the system of 24×24. The blue diamonds denote the Neel phase. The black triangles denote the near-critical region. The red circles denote the PVB phase. The green pentagons denote the stripe phase. (a) From top to bottom, the curves respectively denote the spin correlations at $J_2 = 0.40$, 0.42, 0.44, 0.46, 0.48, 0.50, 0.51, 0.52, 0.53, 0.55, and are respectively shifted by $10^{0.9}$, $10^{0.8}$, $10^{0.9}$, $10^{0.8}$, $10^{0.7}$, $10^{0.6}$, $10^{0.3}$, $10^{0.2}$, $10^{0.1}$, 0.0. (b) Except for the curve of green stars, from bottom to top, the curves respectively denote the spin correlations at $J_2 = 0.58$, 0.60, 0.62, 0.64, 0.66, 0.68, 0.70, and are respectively shifted by $10^{0.2}$, $10^{0.4}$, $10^{0.6}$, 0.0, $10^{0.1}$, $10^{0.2}$, $10^{0.3}$.

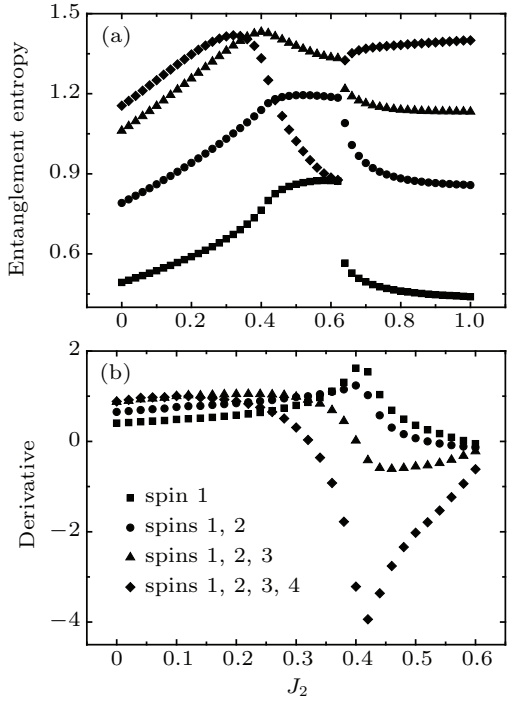

Fig. 6. (a) Entanglement entropy (EE) and (b) its first order derivative on a system of 24×24. The squares, circles, triangles, diamonds respectively denote the EE (first order derivative of EE) of spin 1; spins 1, 2; spins 1, 2, 3; spins 1, 2, 3, 4 in the embedded cluster.

Moreover, the spin energy curves (Fig. 3) also indicate that this phase transition is continuous. To support this, we calculate the entanglement entropy (EE) and its first order derivative in Fig. 6. If we divide the system into two parts A and B, the EE between these two parts is defined as $S = -\mathrm{Tr}(\rho_\mathrm{A} \log_2 \rho_\mathrm{A})$, where $\rho_\mathrm{A} = \mathrm{Tr}_\mathrm{B}(\rho_\mathrm{AB})$ is the reduced density matrix of part A. We embed a cluster. Part A is spin 1 (squares in Fig. 6); or spins 1, 2 (circles in Fig. 6); or spins 1, 2, 3 (triangles in Fig. 6); or spins 1, 2, 3, 4 (diamonds in Fig. 6) of the embedded cluster (Fig. 1). Part B is the rest of the system. A discontinuity or singularity in the EE indicates a first order quantum phase transition, and a peak in the derivative of the EE indicates a continuous quantum phase transition.[13] All the derivatives of EE peak at $J_2 \approx 0.42$ (Fig. 6(b)). This indicates that the phase transition from the Neel phase to the intermediate phase is continuous. By contrast, the spin correlations have a sudden change in the transition from the PVB phase to the stripe phase (Fig. 5(b)). This indicates that this phase transition is a first order one. This is also supported by the discontinuity or singularity of the EE (Fig. 6(a)).

If we embed 6 spins at the top left corner of 6 horizontally consecutive clusters as mentioned above, we measure the spin correlations for every other site (cycles, inset of Fig. 5(a)). To optimize the resolution, we embed 6 consecutive spins at the top of 3 horizontally consecutive clusters on a system of 12×12, and measure the spin correlations (squares, inset of Fig. 5(a)). The spin correlations obtained by these two embedding types are similar (inset of Fig. 5(a)). The spin correlations discussed above in the stripe phase are along its stripes. We also calculate the spin correlations vertical to the stripes at $J_2 = 0.7$ (green stars in Fig. 5(b)). The curve is shifted by $10^{-0.3}$. The distant spin correlations along both directions are strong. In Ref. [35], the static spin structure factors, which are Fourier transformation of the spin correlations, have very sharp peaks in the stripe phase of the square lattice. These sharp peaks indicate strong distant spin correlations. This is consistent with our results.

3.2. Dimer correlation

To shed light on the structures of different phases, we calculate the dimer correlation $DC = \langle \boldsymbol{D}_i^\alpha \cdot \boldsymbol{D}_j^\beta \rangle$, where $\boldsymbol{D}_i^\alpha = \boldsymbol{S}_i \cdot \boldsymbol{S}_{i+\alpha}$, $\boldsymbol{S}_i$ and $\boldsymbol{S}_{i+\alpha}$ are spin operators. In this definition, $\boldsymbol{D}_i^\alpha$ is a dimer which is a nearest neighbor bond on the square lattice. We choose one reference dimer (the line in ellipse in Fig. 7), and calculate the correlations between it and the other dimers in a system of 24×24. In Fig. 7, some dimer correlations are labelled by numerical values. If we label all the dimer correlations with numerical values, the labels will overlap with each other. The thicknesses of lines denote the

strengths of dimer correlations. One can judge the dimer correlations by the thicknesses. Figure 7(c) shows the dimer correlations in the intermediate phase at $J_2 = 0.55$. Every four spins look like to form into a plaquette. The four dimers in a plaquette have the same positive correlations with the reference dimer. This signals the PVB pattern at $J_2 = 0.55$. The inter-plaquette dimer correlations are significantly weaker than the intra-plaquette ones. There is no obvious decaying of dimer correlations in the intermediate phase at $J_2 = 0.55$ (Fig. 7(c)). The dimer correlations look like to maintain a nearly constant value. This may indicate VBS order. Or conservatively, at a minimum, the result indicates that it at least has a (weak) VBS order at $J_2 = 0.55$. Based on these, we consider the region ($0.51 \lesssim J_2 \lesssim 0.62$) as PVB. Consistently, Gong *et al.*[16] also found PVB in this region. We cannot see obvious difference between the dimer correlations at $J_2 = 0.45$ (Fig. 7(b)) and $J_2 = 0.55$ (Fig. 7(c)). Distant spin correlations (Fig. 5) are more sensitive than dimer correlations (Fig. 7) to the phase transition between the near-critical region and the PVB. In Fig. 7(d), at $J_2 = 0.8$, in the stripe phase, the horizontal dimers have positive correlations with the reference dimer. The vertical dimers have negative correlations with the reference dimer. They form stripes. In Fig. 7(a), at $J_2 = 0.2$, in the Neel phase, all the dimers have positive correlations with the reference dimer.

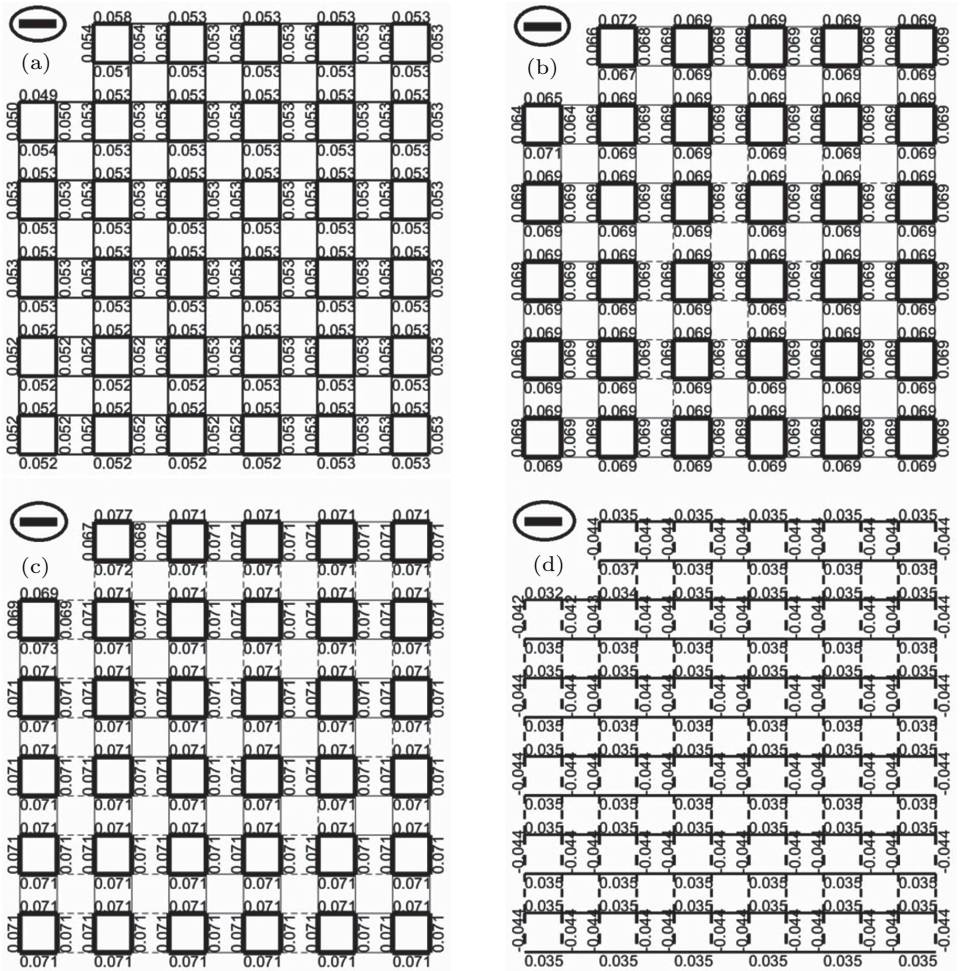

Fig. 7. Dimer correlations on a 24×24 system for different J_2 values: (a) ($J_2 = 0.2$) in the Neel phase, (b) ($J_2 = 0.45$) and (c) ($J_2 = 0.55$) in the intermediate phase, (d) ($J_2 = 0.8$) in the stripe phase. The reference dimer is denoted by the line in ellipse. Negative (positive) correlations are represented by dashed (solid) lines. One cluster is embedded. The reference dimer is in the embedded cluster.

4. Summary

We propose an optimized CDMET, and treat the spins far away from the impurity in the similar way of mean field theory. The accuracy is the same as before. We use the new CDMET to study distant correlations on large systems. In the intermediate phase, the spin correlations gradually tend to decay exponentially as a function of distance. The small region ($0.43 \lesssim J_2 \lesssim 0.50$) is considered as a near-critical region. The spin correlations indicate that this small near-critical region may be a mixed phase (Neel phase with VBS modulation). We find that, at $J_2 = 0.55$, every four spins form into a plaquette. This signals the PVB pattern. The PVB takes place in $0.51 \lesssim J_2 \lesssim 0.62$. In the PVB phase, the spin correlations decay exponentially. The spin correlations, the EE, and the spin energy indicate that the phase transition from the Neel phase

to the intermediate phase is continuous.

References

[1] Wang L and Sandvik A W 2018 *Phys. Rev. Lett.* **121** 107202
[2] Zhang H and Lamas C A 2013 *Phys. Rev. B* **87** 024415
[3] Chen Y, Xie Z Y and Yu J F 2018 *Chin. Phys. B* **27** 080503
[4] Chen J, Liao H J, Xie H D, Han X J, Huang R Z, Cheng S, Wei Z C, Xie Z Y and Xiang T 2017 *Chin. Phys. Lett.* **34** 050503
[5] Liu J L and Liang J Q 2019 *Chin. Phys. B* **28** 110304
[6] Tan X D, Jin B Q and Gao W 2013 *Chin. Phys. B* **22** 020308
[7] Chen S R, Xia Y J and Man Z X 2010 *Chin. Phys. B* **19** 050304
[8] Zhu X and Tong P Q 2008 *Chin. Phys. B* **17** 1623
[9] Bao A, Chen Y H and Zhang X Z 2013 *Chin. Phys. B* **22** 110309
[10] Knizia G and Chan G K L 2012 *Phys. Rev. Lett.* **109** 186404
[11] Bulik I W, Scuseria G E and Dukelsky J 2014 *Phys. Rev. B* **89** 035140
[12] Chen Q, Booth G H, Sharma S, Knizia G and Chan G K L 2014 *Phys. Rev. B* **89** 165134
[13] Fan Z and Jie Q L 2015 *Phys. Rev. B* **91** 195118
[14] Qin J B, Jie Q L and Fan Z 2016 *Computer Physics Communications* **204** 38
[15] Gunst K, Wouters S, Baerdemacker S D and Neck D V 2017 *Phys. Rev. B* **95** 195127
[16] Gong S S, Zhu W, Sheng D N, Motrunich O I and Fisher M P A 2014 *Phys. Rev. Lett.* **113** 027201
[17] Gelfand M P, Singh R R P and Huse D A 1989 *Phys. Rev. B* **40** 10801
[18] Jiang H C, Yao H and Balents L 2012 *Phys. Rev. B* **86** 024424
[19] Murg V, Verstraete F and Cirac J I 2009 *Phys. Rev. B* **79** 195119
[20] Darradi R, Derzhko O, Zinke R, Schulenburg J, Krüger S E and Richter J 2008 *Phys. Rev. B* **78** 214415
[21] Chandra P and Doucot B 1988 *Phys. Rev. B* **38** 9335
[22] Read N and Sachdev S 1989 *Phys. Rev. Lett.* **62** 1694
[23] Takano K, Kito Y, Ono Y and Sano K 2003 *Phys. Rev. Lett.* **91** 197202
[24] Mezzacapo F 2012 *Phys. Rev. B* **86** 045115
[25] Yu J F and Kao Y J 2012 *Phys. Rev. B* **85** 094407
[26] Li T, Becca F, Hu W and Sorella S 2012 *Phys. Rev. B* **86** 075111
[27] Wang L, Poilblanc D, Gu Z C, Wen X G and Verstraete F 2013 *Phys. Rev. Lett.* **111** 037202
[28] Hu W J, Becca F, Parola A and Sorella S 2013 *Phys. Rev. B* **88** 060402
[29] Doretto R L 2014 *Phys. Rev. B* **89** 104415
[30] Henelius P and Sandvik A W 2000 *Phys. Rev. B* **62** 1102
[31] Wang L, Gu Z C, Verstraete F and Wen X G 2016 *Phys. Rev. B* **94** 075143
[32] Sirker J, Zheng.W, Sushkov O P and Oitmaa J 2006 *Phys. Rev. B* **73** 184420
[33] Jongh M S L D C D, Leeuwen J M J V and Saarloos W V 2000 *Phys. Rev. B* **62** 14844
[34] Sushkov O P, Oitmaa J and Zheng W 2001 *Phys. Rev. B* **63** 104420
[35] Morita S, Kaneko R and Imada M 2015 *J. Phys. Soc. Jpn.* **84** 024720